ELSEVIER

Journal of Alloys and Compounds 218 (1995) 237–243

Journal of ALLOYS AND COMPOUNDS

High-temperature oxidation of one- and two-component metallic systems studied by in-situ X-ray absorption spectroscopy

Massimo Tomellini [a], Ivan Davoli [b], Daniele Gozzi [c]

[a] *Dipartimento di Scienze e Tecnologie Chimiche, Università di Roma 'Tor Vergata', Via della Ricerca Scientifica, 00133 Roma, Italy*

[b] *Dipartimento di Matematica e Fisica, Università di Camerino, 62032 Camerino, Italy*

[c] *Dipartimento di Chimica, Università di Roma 'La Sapienza', Ple. Aldo Moro 5, 00185 Roma, Italy*

Received 20 June 1994; accepted 31 August 1994

Abstract

A high-temperature oxidation technique by in-situ characterization of the oxide growth is presented. The technique has been utilised to study the oxidation of one- and two-component systems. Results on the oxidation of Ni and Ni–Fe solid solution are reported for low values of the oxygen partial pressure, namely 0.3 Pa. X-Ray absorption spectroscopy (XAS) measurements at the Fe and Ni K-edges were made in fluorescence mode and after each oxidation step. The atomic selectivity of XAS makes this technique particularly suitable when studying selective oxidations. As indicated by the spectroscopic data, the oxidation of the Fe–Ni alloy mainly involves iron cations, and it leads to the growth of iron oxide, the formation of the ferrite being unfavourable. The oxidation kinetics are also obtained by an appropriate analysis of the spectroscopic data, and the parabolic rate constants have been evaluated. These results indicate that the technique is particularly suitable for studying the hot corrosion of oxide film too thick for common surface spectroscopy and too thin for conventional thermogravimetric technique.

Keywords: Oxidation; Metallic systems; X-ray absorption spectroscopy

1. Introduction

High-temperature oxidation of metal and alloy surfaces has been, for many years, the subject of considerable research because of its basic scientific interest and technological importance. Since the pioneering work of Tammann [1], many papers have been devoted to the study of both the oxidation kinetics and the structure of oxides formed at high temperatures [2,3]. An extended literature has been especially dedicated to the kinetics of high-temperature oxidation of metals in air or in pure oxygen. The scenario, however, changes considerably when one looks for oxidation data taken at low oxygen partial pressures. Also for quite common metals such as nickel, copper and iron it is difficult to find a sufficient quantity of data in those experimental conditions. Nevertheless, there are a growing number of applications where the behaviour of metallic materials vs. oxidation under low oxygen partial pressure conditions has to be studied [4].

The characterization of the oxide overlayer is generally performed, in an accurate way, by non-surface-sensitive techniques such as X-ray or electron diffraction. This is because oxide thicknesses of the order of magnitude of a few microns are usually formed at high temperature. In the case of the oxidation of multicomponent systems, however, the diffraction method for determining lattice constants could not be accurate enough to distinguish between different structures. As an example, it was established in the literature that the oxidation of Ni/Fe alloys in air can lead to the formation of nickel ferrite ($NiFe_2O_4$) or iron ferrite (Fe_3O_4). These ferrites crystallize in the spinel structure and have similar lattice constants, namely 8.34 Å and 8.37 Å, respectively. The identification of one of these two structures by X-ray diffraction is therefore not straightforward. In this case a spectroscopic technique that is sensitive to the atomic number around a particular cation site is highly desirable in order to distinguish between iron and nickel sites octahedrally and tetrahedrally coordinated to oxygen, respectively.

In our previous paper [5] an in-situ technique was presented that should allow the study of both the oxidation kinetics and oxide overlayer structure during the high-temperature oxidation of metal surfaces. We performed oxide characterization by XAS, which is

SSDI 0925-8388(94)01396-9

known to be sensitive to the local structure around the specific atomic species. Since XAS measurements are performed in fluorescence mode, thin samples or dilute specimens are required by this technique.

In this paper we present experimental results on the oxidation of one- and two-component systems, at high temperature and low oxygen partial pressure, by the above-mentioned technique. Particular attention is devoted to the selectivity of the XAS towards each atomic species of the specimens, which allowed us to follow, separately, the oxidation of each component of the alloy. An attempt to perform a joint study of the oxidation kinetics and oxide structure during the oxidation of both nickel foil and Ni/Fe solid solution is presented.

2. Experimental details

Since the experimental apparatus has been described elsewhere [5] only a brief description is here summarized. The experimental set-up is shown in Fig. 1 and is constituted by a spectroscopic chamber that is located in the "hard X-ray" beam line of ADONE, the storage ring of the National Laboratories of Frascati,

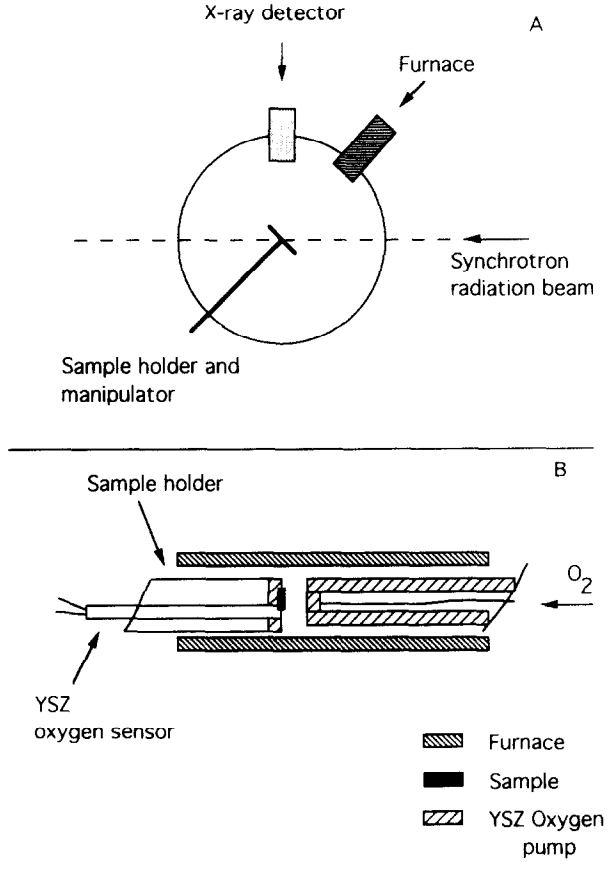

Fig. 1. (A) Schematic view of the experimental set-up for the in-situ characterization of oxide growth on parent metal. (B) Details of the sample holder, oxygen pump and microfurnace.

operating at 1.5 GeV and 50 mA. A Si(111) channel-cut monocrystal was used as monochromator with an energy resolution, in the energy region explored, of 0.5 eV. The data acquisition was assisted by a PDP/11 computer. In the spectroscopic chamber a manipulator drives the sample holder from the centre of the chamber, where the spectroscopic measurements are collected, into a micro furnace that can reach temperatures up to 1100 °C. The sample oxidation is performed in the furnace, and the oxygen is supplied to the sample surface through a YSZ (yttria-stabilized zirconia) oxygen pump operating in galvanostatic mode. Spectroscopic measurements are recorded in the fluorescence mode at room temperature after each oxidation step. A YSZ oxygen sensor is located in the sample holder, just beneath the surface of the sample, to measure the oxygen partial pressure under which oxidations are performed.

3. Results and discussion

3.1. Spectrum analysis

The method adopted to process the fluorescence spectra has been described in our previous work [5] and, as summarized in what follows, is based on the decoupling of oxide and metal spectra whose superposition gives rise to the measured fluorescence intensity. In particular, we consider the oxide growth according to the reported experimental set-up as due to the successive current steps applied to the oxygen pump. S_j denotes the intensity of the cation K-edge recorded after the jth galvanostatic step, whereas for quantities like intensity, site numbers, oxidation time related to the jth oxidation step, use is made of the subscript $j-1,j$. The following relation was obtained

$$S_j=\sum_i\left[\frac{n_{i-1,i}}{N_0}\right]S_{i-1,i}(\mathrm{MO})+\left[1-\sum_i\frac{n_{i-1,i}}{N_0}\right]S(\mathrm{M}) \qquad (1)$$

where n is the number of cation sites in the oxidized state, N_0 the whole number of sites, S(MO) and S(M) the intensities of the oxide and the pure metal spectra, respectively. The sum over i runs from 1 to j. This expression is justified on the basis of the fluorescence counting rate obtained in the case of thin samples ($\mu d \ll 1$) [6]. It reads

$$I_f=I_0\epsilon\mu_i(E)l_0\left[\frac{\Omega}{4\pi}\right] \qquad (2)$$

where I_0 (I_f) is the incident (measured) intensity, ϵ the radiative probability, $\mu_i(E)$ the adsorption coefficient for the ith species, E the energy of the incident radiation, l_0 the sample thickness and Ω the outcoming solid angle. By considering the oxidized surface as a two-

component system because of the presence of cations in both oxidized and metallic states, Eq. (2) is rewritten according to

$$I_f = I_0 \epsilon \left[\frac{\Omega}{4\pi S_0}\right][\sigma_{ox} n + \sigma_m (N_0 - n)] \quad (3)$$

where σ_{ox} and σ_m are the adsorption cross-sections for the cation in the oxide and metal, respectively, and S_0 is the sample area. Eq. (3) also holds in the case of an island growth oxidation mechanism. Indeed, by considering the formation of oxide islands at the metal surface, the whole fluorescence intensity for the metal K-edge is given by

$$I_f = \left\{\sum_k s_k \mu_{ox} d_k + \sum_k s_k \mu_m l_k + \left(S_0 - \sum_k s_k\right)\mu_m d_0\right\} \frac{I_0 \epsilon}{S_0}\left(\frac{\Omega}{4\pi}\right) \quad (4)$$

where the sums are over the island population, s_k is the area of the kth island with average thickness d_k, l_k is the thickness of the metal hindered by the kth island, and d_0 is the initial thickness of the metal film. By using $\mu = \rho\sigma$ in Eq. (4) and considering that $n = \rho_{ox} \Sigma s_k d_k$, Eq. (3) is easily derived.

In the case of oxide film growth, the ratio n/N_0 is given by

$$\frac{n}{N_0} = \frac{\rho_{ox} l}{\rho_m X_0} \quad (5)$$

where ρ_{ox} and ρ_m are the cation densities in the oxide and metal phases, respectively, l is the thickness of the oxide layer and X_0 the initial thickness of the metal foil. Under this assumption, the evaluation of the $\Delta S_j = S_j - S_{j-1}$ term is obtained from Eq. (1) as follows

$$\Delta S_j = x_{j-1,j} \Delta S_{j-1,j} \quad (6)$$

where $x = \rho_{ox} l/(S_m X_0)$ and $\Delta S_{j-1,j} = S_{j-1,j} - S(\mathrm{M})$. If one assumes that the oxide structure does not change during the growth process up to the nth galvanostatic step when the sample oxidation reaches completion, the following relation holds

$$\Delta S_{j-1,j} = \Delta S = S_n - S(\mathrm{M}) \quad (7)$$

and the oxidation kinetics is consequently obtained using Eq. (6):

$$x_{j-1,j} = \Delta S_j / \Delta S \quad (8)$$

or, in terms of the oxide thickness, according to

$$d_{j-1,j} = \frac{\rho_m X_0 \Delta S_j}{\rho_{ox} \Delta S} \quad (9)$$

As previously pointed out [5], the growth kinetics can be determined by considering only a selected energy region of the XAS spectrum that is unaffected by a change of the oxide stoichiometry. In the case of Ni oxidation, for example, it was shown that nickel vacancies induce extra holes at the oxygen sites in NiO. Accordingly, the spectral region close to the K-adsorption edge of the cation is unaffected by such a change in the structure. On this basis, the x value can be determined as follows

$$x_j = \frac{\int_{E_1}^{E_2} [I_m - I_j] dE}{\int_{E_1}^{E_2} [I_m - I_{ref}] dE} \quad (10)$$

where $E_1 - E_2$ is the selected spectral range, I_m, I_j and I_{ref} are the spectral intensities of metal foil, sample after j oxidation steps and reference oxide, respectively. Through the knowledge of the x value it is possible to "reconstruct" the oxide spectra, S_j(MO), in the whole experimental range of the energies. By using Eq. (1) it follows that

$$S_j(\mathrm{MO}) = S(\mathrm{M}) - \frac{[S(\mathrm{M}) - S_j]}{x_j} \quad (11)$$

Therefore, under the assumption of a *layer-by-layer* growth mechanism of the oxide, it is possible to extract jointly information on the oxidation kinetics and oxide structure.

3.2. Oxidation of one-component system

The proposed experimental technique was first tested on a one-component system, namely a nickel foil 2 μm thick. This low thickness value allows the approximation reported in Eq. (3) to be satisfied with an accuracy of 85%, as evaluated on the basis of the value of the K-edge cross-section reported in the literature. The Ni oxidation was performed at a temperature of 750 °C, and the steady state of the oxygen partial pressure value, measured by the sensor close to the sample was, on average, 0.17 Pa. In particular, the sample was submitted to three galvanostatic steps of 15, 30 and 52 min in which the oxygen pump was polarized with current values of 75 and 100 mA, respectively. The blank value of the oxygen partial pressure in the chamber was about 10^{-4} Pa. By assuming the ionic transport number in the solid electrolyte to be equal to 1, the oxygen flux at $I = 50$ mA was also calculated to be of the order of 10^{-6} mole cm^{-2} s^{-1}.

As an example, in Fig. 2A is reported the sensor e.m.f. recorded during the third oxidation step for a period long enough to allow the curve of the oxygen partial pressure to reach the steady-state condition. The oxygen partial pressure is obtained from the knowledge of the e.m.f., E, based on the Wagner equation calculated at $t_i = 1$: $P_{O_2} = P_{ref} \exp(4FE/RT)$, P_{ref} being

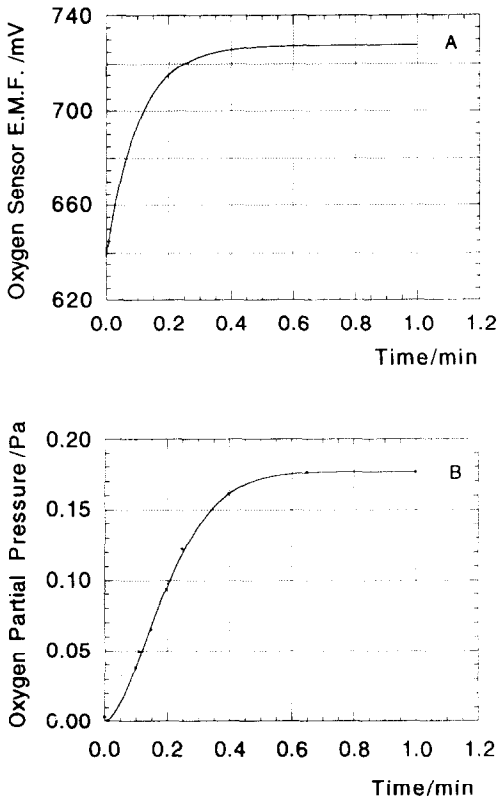

Fig. 2. Transients of (A) the sensor e.m.f. and (B) of the oxygen partial pressure at the nickel surface recorded during a typical oxidation step.

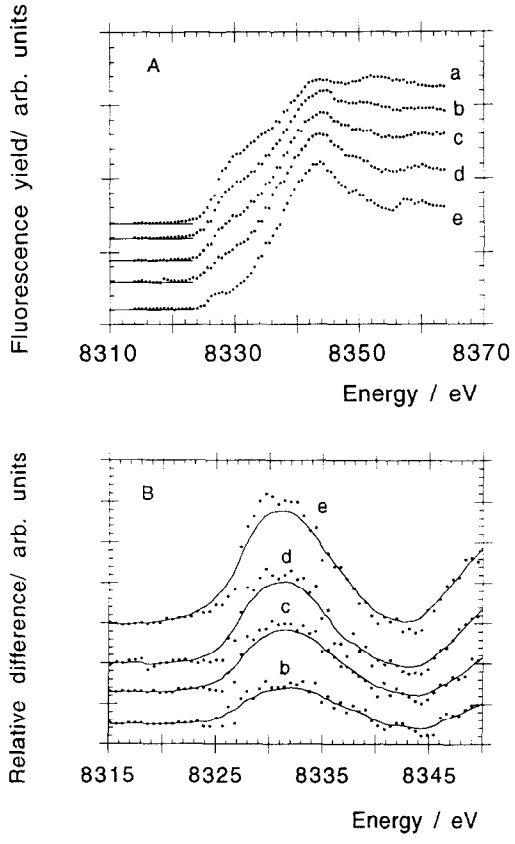

Fig. 3. (A) Fluorescence yields at the Ni K-edge collected after thermal treatment of the microfoil in vacuum (spectrum (a)) and after three successive oxidation steps ((b)–(d)). Curve (e) is the spectrum of the reference nickel oxide, namely a Ni sheet oxidized in air for 10 min at 800 °C. (B) Differences between the spectrum of the unoxidized surface (a) and the spectra (b)–(e).

the oxygen partial pressure at temperature T existing in the Fe–wüstite coexistence mixture at the thermodynamic equilibrium (Fig. 2B) [7].

The experimental data are shown in Fig. 3A. The fluorescence spectra at the Ni K-edge have been recorded after each galvanostatic step. In particular, curve (a) was obtained after thermal treatment in vacuum ($I=0$, $T=800$ °C, $\Delta t=10$ min), curves (b)–(d) after the oxidation steps, and spectrum (e) is the fluorescence spectrum of the Ni foil completely oxidized in air at $T=800$ °C. According to Fig. 3A, we observe that modifications in the spectra mainly occur at about 8330 eV. The oxidation kinetics is extracted from the fluorescence spectra by using Eq. (10). The spectral difference $(I_m - I_j)$ is reported in Fig. 3B for the selected region of the spectrum ($E_1=8325$ eV, $E_2=8340$ eV). On the assumption of a layer-by-layer growth mechanism, the x parameter obtained from Eq. (10) is related to the oxide thickness. This is reported in Fig. 4, where the $l(t)$ kinetics has been extracted from the experimental x values according to the expression $l(t)=\rho_m X_0 x(t)/\rho_{ox}$, $l(t)$ being the oxide thickness.

It is worth remembering that several works have been devoted to the study of the growth mechanism of oxide scale on metals at high temperature [8]. The basic assumption in the Wagner model is that the transport of reacting species across the *oxide film* is

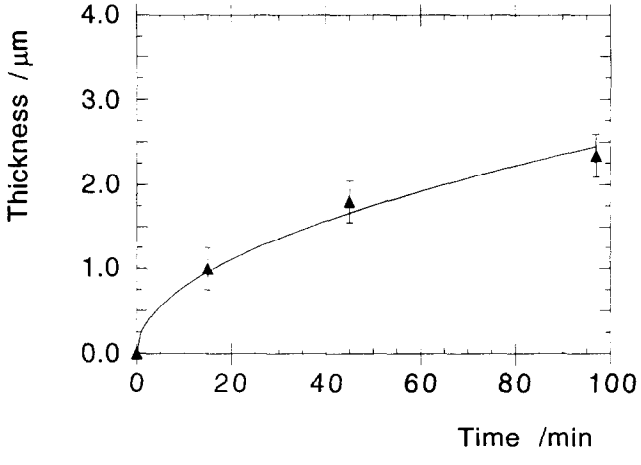

Fig. 4. Oxidation kinetics of nickel foil 2 μm thick as revealed by XAS measurements. The oxidation was performed at a temperature of 750 °C and at an oxygen partial pressure of 0.17 Pa. By a fitting procedure the parabolic rate constant was evaluated to be $(5.2\pm0.3)\times10^{-12}$ cm^2 s^{-1}.

rate-determining in the whole reaction of oxidation [4,8]. The model leads to a parabolic growth law for the oxide thickness, $l(t)=(2Kt)^{1/2}$, where the rate con-

stant K is a function of both temperature and oxygen partial pressure.

As appears from Fig. 4, the experimental kinetics is well described by a parabolic growth law with a rate constant equal to 5.2×10^{-12} cm^2 s^{-1}. This figure is in quite good agreement with the values previously obtained, where K was found to lie in the range 10^{-12} to 10^{-13} cm^2 s^{-1} for temperature values in the interval 700–800 °C, respectively, and at $P_{O_2}=10^{-5}$ atm [9–11]. Because these values are strongly dependent on the grain size of the polycrystalline sample as well as on the metal surface pre-treatment, they are only indicative of the order of magnitude of the rate constant.

The treatment of the spectroscopic data is sensitive to the growth mechanism of the oxide phase. The proposed method for data analysis unambiguously indicates that nickel oxidation mainly occurs through the formation of an oxide film, a result that is also in agreement with several studies previously performed on the Ni–O_2 system. The "reconstructed" spectrum of the NiO layer after the third galvanostatic step has been reported in Fig. 5 (curve (b)), jointly with the NiO reference spectrum (a). The curve has been obtained by applying Eq. (11) to the whole energy range, while the x_j value has been extracted in a reduced energy range near to the adsorption edge. As appears from Fig. 5, the comparison between the two curves indicates that the structure of the oxide layer does not deviate significantly from the reference oxide.

3.3. Alloy oxidation

The oxidation of an iron–nickel alloy has also been studied using the computation technique described in Section 3.1. A polycrystalline alloy Fe(64%)–Ni(36%) 8 μm in thickness (Goodfellow) has been oxidized with three galvanostatic steps ($I=75$ mA) at the constant temperature of 660 °C and for an average value of the oxygen partial pressure of 0.3 Pa. The selectivity of the XAS towards the different atomic species of the sample allowed us to study, separately, the oxidation of both Ni and Fe cations. This is shown in Figs. 6A and 6B, where the K edges of Fe and Ni are reported, respectively, after the oxidation steps (curves (b)–(d)) and for the unoxidized alloy (curve (a)). In Fig. 6A is also reported the reconstructed spectra of iron as obtained on the ground of Eq. 11 (curve *e*).

As appears from the spectroscopic data, no change occurs in the Ni K-edge spectra during the oxidation process, within the resolution dictated by the S/N ratio of the measurements, whereas a *kinetics* is observed at the Fe K-edges. In particular, this is shown in Fig. 7A for the spectrum difference, $I_{Fe}-I_j$ for $j=1$–4, and in Fig. 7B in terms of the $l(t)$ kinetics for the formation of the FeO phase (see below). The kinetics is found to be in agreement with a parabolic growth law with a rate constant equal to 4.5×10^{-11} cm^2 s^{-1}. It is worth remembering that $Fe_{1-x}O$ is non-stoichiometric because of the formation of defect clusters, i.e. cation vacancy aggregation [12]. The formation of the {4:1} complex

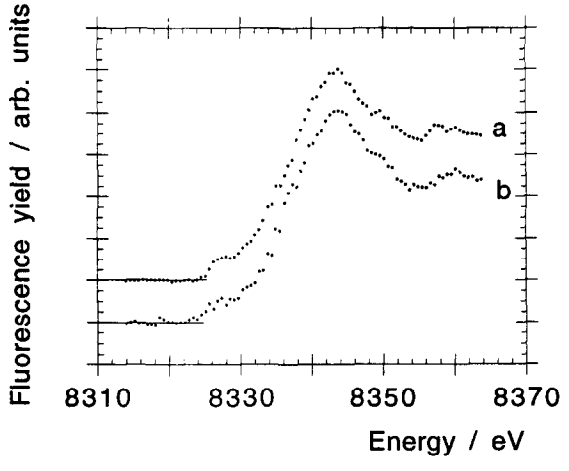

Fig. 5. Comparison between the Ni K-edge XAS spectrum of the reference NiO (curve (a)) and the *reconstructed* spectrum of the oxide overlayer (curve (b)).

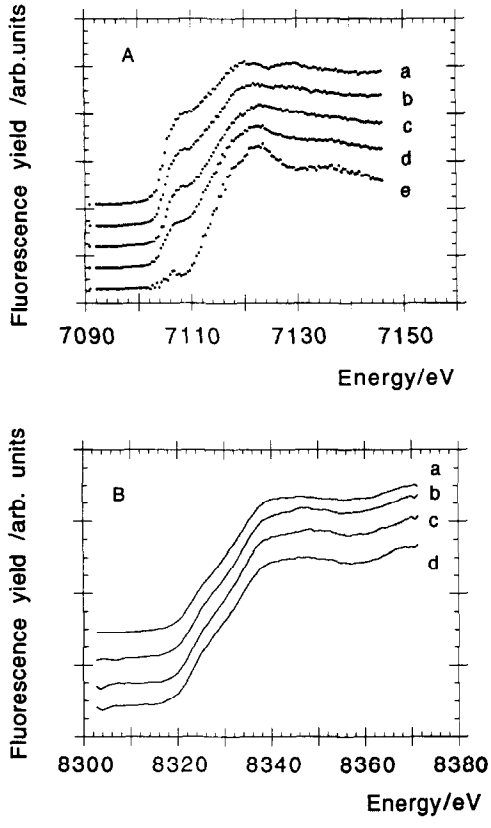

Fig. 6. Fluorescence yields during oxidation at 660 °C and 0.3 Pa oxygen pressure of the Fe(64%)-Ni(36%) solid solution (curve (a), after thermal treatment of the sample in vacuum; curves (b)–(d), after three galvanostatic steps): (A) iron K-edge (curve (e), reconstructed spectrum of the oxide overlayer, according to the proposed data treatment); (B) nickel K-edge.

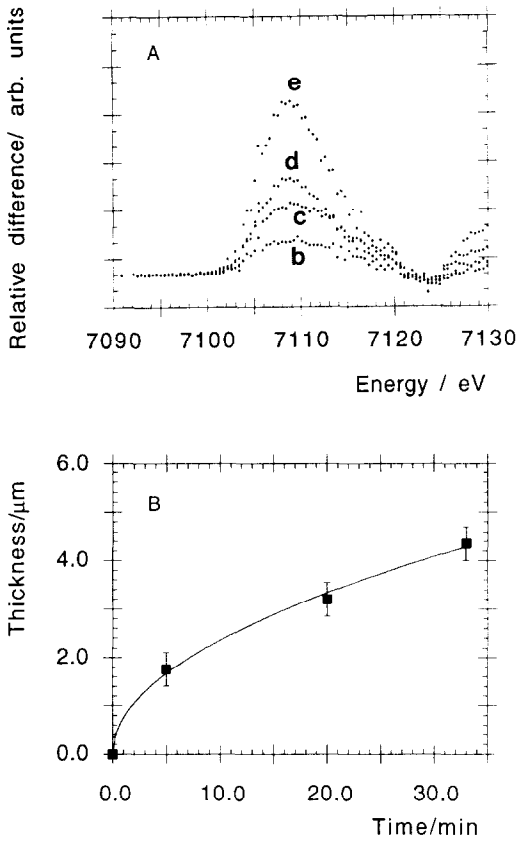

Fig. 7. (A) Spectral differences between the fluorescence yields at the Fe K-edges of the unoxidized surface and of the oxidized ones (spectra (b)–(e)). (B) Oxidation kinetics derived by the spectrum differences of (A): the parabolic rate constant was found to be $(4.5 \pm 0.3) \times 10^{-11}$ cm^2 s^{-1}.

defect (4 vacancies + 1 interstitial iron tetrahedrally coordinated) may be written in terms of the following reactions

$$3/2O_2 \longleftrightarrow 3V''_{Fe} + 3O_0 + 6h^{\cdot}$$

and a Frenkel defect pair

$$Fe_{Fe} \longleftrightarrow Fe_i^{\cdot\cdot} + V''_{Fe}$$

The direct, overall formation of the complex is written as

$$Fe_{Fe} + 3/2O_2 \longleftrightarrow \{4:1\}''' + 3h^{\cdot} + 3O_0$$

where $Fe_i^{\cdot\cdot}$ stands for a double-charged interstitial cation, V''_{Fe} for double-charged iron vacancies, Fe_{Fe} for a cation in its regular position, $h^{\cdot}$ for a hole and O_0 for an oxygen atom in a regular lattice position. The rate constant K is proportional to the product $D_{Fe} t_e y$, where D_{Fe} is the diffusion coefficient of iron in FeO, t_e is the electronic transport number, and y is the mole fraction of defects. By considering $D_{Fe} \approx 10^{-9}$ cm^2 s^{-1} [4], $t_e = 1$, the value of y has been estimated to be 0.01.

The oxidation of the iron–nickel alloys in the temperature interval 500–1100 °C has been extensively studied in the whole range of the alloy composition and at an oxygen partial pressure of 0.2 atm [13–16]. Both the oxidation kinetics and the oxide microstructure were studied; in particular, the former by means of thermogravimetric measurements and the latter through metallographic and electron-diffraction techniques [13,14]. The oxidation kinetics was found to be parabolic and the oxide structure dependent on the alloy composition. In particular, for the Ni(40%)-Fe(60%) austenitic solid solution, the oxidation rate constant was found to be 1.27×10^{-12} g^2 cm^{-4} s^{-1} for oxidations of about 60 min duration at $T = 600$ °C. Also, the film was constituted by a Fe–Ni spinel and by the Fe_2O_3 oxide on the atmosphere side [16]. In fact, above 600 °C the iron oxide reacts with the NiO to form the spinel $Ni_xFe_{3-x}O_4$; when stoichiometric, the composition of the spinel is $NiFe_2O_4$.

The measurements we present refer to the alloy oxidations at lower values of the oxygen partial pressure compared to those previously reported [13]. In fact, in our experiment the average P_{O_2} value during each oxidation step was 0.3 Pa. The spectra reported in Fig. 6B unambiguously show that neither the Ni oxidation state nor the Ni local order is changed during the alloy oxidation, within the resolution of the present technique. This implies a detection limit for the thickness of the NiO layer of about (2000 Å) 200 nm [5]. In contrast, iron is oxidized as indicated by the spectra of Figs. 6A and 7A. The oxidized phase can be identified with the FeO oxide on the basis of the reconstructed spectrum (e) of Fig. 6A. The energy difference between the Fe absorption K-edge in the metal and the position of the main line in the XAS spectrum of the metal K-edge in the oxide was found to be 12.5 eV and 15 eV in the case of FeO and Fe_2O_3, respectively [17]. The evaluation of the same quantity on the basis of spectra (a) and (e) of Fig. 6A gives 12.6 eV where the K-edge of the metal is at 7109 eV. In addition, this result is in agreement with a previous study [18] performed in our lab, on the stability of the iron oxide phases at low oxygen activity.

4. Conclusions

A high-temperature oxidation technique has been utilised to study the oxidation of one- and two-component systems. In the case of alloy specimens, the selectivity of XAS to the atomic species selected in the absorption process allowed us to follow, separately, the oxidation of each component in the alloy. In particular, we studied the oxidation of a Ni–Fe solid solution, at high temperature and low oxygen partial pressures. On the basis of the XAS measurements, the formation of the nickel ferrite at the oxide–O_2 interface was ruled out and the growth of a FeO overlayer established. This is within the detection limit of the

technique, i.e. of about 0.2 μm in thickness. Furthermore, the parabolic rate constants for the oxidation of Ni and Ni–Fe systems were extracted by an appropriate analysis of the spectroscopic data. The technique presented seems to be promising for studying the oxidation of dilute metallic solution, a few micrometres thick.

Acknowledgements

The authors wish to thank the CSM (Centro Sviluppo Materiali, Roma) and PULS-INFN LNF (Laboratori Nazionali di Frascati) for the joint financial support given to realize the high-temperaure system on the *hard X-ray* beam-line facility.

References

[1] G. Tammann, *Z. Anorg. Allgem. Chem., 111* (1920) 78.
[2] W.W. Smeltzer and D.J. Young, *Progr. Solid State Chem., 10* (1975) 17.
[3] K.R. Lawless, *Rep. Progr. Phys., 37* (1974) 231.
[4] P. Kofstad, in *High Temperature Corrosion*, Elsevier Applied Science, London and New York, 1988.
[5] M. Tomellini, D. Gozzi and I. Davoli, *J. Mater. Chem., 2* (1992) 754.
[6] J. Jaklevic, J.A. Kirby, M.P. Klein, A.S. Robertson, G.S. Brown and P. Eisenberger, *Solid State Comm., 23* (1977) 679.
[7] *JANAF Thermochemical Tables*, suppl. *J. Phys. Chem. Rev. Data, 4* (1975) 156.
[8] A.T. Fromhold Jr., *Theory of Metal Oxidation*, North-Holland, Amsterdam, 1980.
[9] E.A. Gulbransen and K.F. Andrew, *J. Electrochem. Soc., 101* (1954) 128.
[10] K. Fueki and J.B. Wagner Jr., *J. Electrochem. Soc., 112* (1965) 384.
[11] M.L. Volpe and J. Reddy, *J. Chem. Phys., 53* (1970) 1117.
[12] C.R.A. Catlow and B.E.F. Fender, *J. Phys. C, 8* (1975) 3267.
[13] R.T. Foley, J.U. Druck and R.E. Fryxell, *J. Electrochem. Soc., 102* (1955) 440.
[14] R.T. Foley, C.J. Guare and H.R. Schmidt, *J. Electrochem. Soc., 104* (1957) 413.
[15] R.T. Foley and C.J. Guare, *J. Electrochem. Soc., 106* (1959) 936.
[16] R.T. Foley, *J. Electrochem. Soc., 109* (1962) 1202.
[17] L.A. Grunes, *Phys. Rev. B, 27* (1983) 2111.
[18] D. Gozzi and P.L. Cignini, *J. Appl. Electrochem., 13* (1983) 221; D. Gozzi and P.L. Cignini, unpublished results.